

A new mechanism in the formation of PET extended-chain crystal

Li Liangbin^a, Huang Rui^{a,*}, Zhang Ling^a, Hong Shiming^b

^aDepartment of Polymer Material Science and Engineering, Sichuan University, Chengdu, Sichuan 610065, People's Republic of China

^bInstitute of Atomic and Molecular Physics, Sichuan University, Chengdu, Sichuan 610065, People's Republic of China

Received 13 May 1999; received in revised form 16 November 1999; accepted 8 May 2000

Abstract

In order to obtain a better understanding of the effect of transesterification in PET extended-chain crystallization, the crystallization behaviors of the PET samples with added catalysts and inhibitors of transesterification have been investigated at high pressure. The catalyst accelerated PET crystallization in two facets: (I) increasing the crystallinity; and (II) accelerating the thickening process of lamellar crystals. On the contrary, the inhibitor hindered crystallization. This indicates that transesterification can promote PET crystallization and improve the formation of extended-chain crystals. The different effects of transesterification to crystallization in amorphous region or molten state and on folded-chain surface of lamellar crystals has also been discussed; it suggested that transesterification between lamellar crystals is more effective for lamellar crystal thickening. © 2000 Elsevier Science Ltd. All rights reserved.

Keywords: Extended-chain crystal; Poly(ethylene terephthalate); Transesterification

1. Introduction

Poly(ethylene terephthalate) (PET) is a semicrystalline polymer composed of crystalline and amorphous regions. A great variety of microstructure can be developed in PET by changing the crystallization conditions [1]. High pressure is one of the interesting methods to affect its structure that has attracted many researchers.

Siegmann et al. [2] reported that high-pressure crystallized PET samples have a high temperature (549 K) and a low temperature (531 K) atmospheric melting points, and that the extended-chain crystals (40–100 nm) can be formed under high pressure. Hiramatus et al. [3] also observed an increase in the melting point to more than 563 K for samples annealed under high pressure. However, Phillips et al. [4] reported that no evidence was found to support the formation of extended-chain crystals under high pressure, and the atmospheric melting point of high-pressure crystallized PET samples decreased with increasing pressure. Recently, a nanocrystalline structure was reported in the high-pressure crystallized PET samples. The thickness of the crystalline lamella was about 10 nm [5]. Thus, it can be seen that the reports about high-pressure crystallized PET have discrepancies.

Recently, we have re-investigated the crystallization

behavior of PET at high pressure and confirmed that the PET extended-chain crystal can be formed during high-pressure crystallization. Their thickness was up to 4.5 μm (about 45 times the average length of the original molecular chains) when crystallization time was only 6 h [6]. Similar results for polyethylene (PE) have also been reported, but the crystallization time was much longer (200 h) [7]. The fast thickening rate possibly suggests that because of the $-\text{COOC}-$ groups present in the polymer chain, the mechanism of an extended-chain crystallization in PET may differ from that proposed for PE. It has been suggested for PE that chain-sliding diffusion is the main factor for the formation of extended-chain crystals [8,9]. A loose-packed hexagonal form, which has been thought as a mobile phase, plays an important role in the polymer crystallization.

Transesterification is often found during atmospheric pressure crystallization and annealing of polyesters [10] and has been reviewed by Porter and Wang [11] for binary polymer blends. Sequential reordering in co-polyesters, influenced by transesterification and crystallization, has also been investigated by Fakirov [12–14]. Kugler and Zachmann [15] and Mcalea [16] have employed small angle neutron scattering to observe the ester-interchange reactions in pure PET samples. The success of this technique is based on the difference in coherent scattering length between hydrogen and deuterium. The former also suggested that transesterification could decrease the number of chain entanglements and promote crystallization.

* Corresponding author. Tel.: +86-28-5403513; fax: +86-28-5220670.
E-mail address: huangrui@pridns.scu.edu.cn (H. Rui).

Table 1
The crystallization conditions and results

Sample	Starting material	Crystallization conditions	Melting point T_m (K)	Melting enthalpy cal/g	Crystallinity X_c (%)
Sample 1	PET +0.4% $(C_6H_5)_3PO_4$	300 Mpa 573 K 90 min	529	15.42	47.97
Sample 2	PET	300 MPa 573 K 90 min	529 542	17.76 1.45	55.25
Sample 3	PET +0.4% $Ti(OC_4H_9)_4$	300 MPa 573 K 90 min	544	28.88	89.85
Sample 4	PET +0.4% $(C_6H_5)_3PO_4$	300 MPa 603 K 90 min	535	20.3	63.32
Sample 5	PET	300 MPa 603 K 90 min	546	23.92	74.42
Sample 6	PET +0.4% $Ti(OC_4H_9)_4$	300 MPa 603 K 90 min	555	24.61	78.54

This work was undertaken in order to obtain a better understanding of the effect of transesterification on a PET extended-chain crystallization. Because the transesterification is difficult to be detected in a simple system, we characterized the effect of transesterification through investigating the effect of a catalyst and inhibitor on the extended-chain crystallization.

2. Experimental

An unoriented commercial PET (Yanshan Petrol. Chem. Co., China) was used as the original material. The molecular weight, calculated from viscosity, was about 18,000. Tetra-butyl titanate $Ti(OC_4H_9)_4$ and triphenyl phosphite $(C_6H_5)_3PO_4$ were used as the catalyst and inhibitor of transesterification, respectively. Carduner et al. [17–18] have reported that organophosphites are inhibitors of ester-exchange reactions. The original PET material was allowed to stand for 36 h at 368 K in vacuum to eliminate moisture and then made into powder (average size about 0.5 mm). The catalyst or inhibitor was blended with the PET powder. High-pressure experiments were carried out with a piston-cylinder high-pressure apparatus [19]. The following procedure for crystallization was used. After loading the

samples, low pressure was applied and the temperature was raised to a predetermined value. After equilibrium was established, the pressure was raised to the desired level. The samples were kept under these conditions for 90 min and then quenched down to ambient conditions. The starting material and crystallization conditions are listed in Table 1.

Calorimetric measurements were performed by using a Perkin–Elmer DSC-2 differential scanning calorimetry (DSC). The degree of crystallinity X_c was obtained from the melting enthalpy ΔH_m by means of the equation

$$X_c = \Delta H_m / \Delta H_m^\circ$$

where ΔH_m° is the melting enthalpy of the ideal crystal, which was assumed to be 135 J g^{-1} according to Starkweather et al. [20]. The calorimeter was calibrated with standard substances, which melt in the range of PET melting.

Fourier transform infrared spectroscopy (FTIR) was performed on a Nicolet 20SXB instrument. The PET powder was blended with KBr and pressed into pellets for FTIR investigation. For microscopy, the samples were fractured at liquid N_2 temperature and then hydrolyzed at 453 K for 90 min to etch the surface. The hydrolysis method is similar to that developed by Miyagi and Wunderlich [10]. The hydrolyzed fracture surface was observed on an AMRAY1845FM scanning electron microscope (SEM). For transmission electron microscopy (TEM) observation, the hydrolyzed fracture surface was also shadowed with platinum, stripped with poly(acrylic acid), and backed with carbon.

3. Results and discussion

The DSC measurements of PET samples crystallized at 300 MPa and 573 K for 90 min are shown in Fig. 1. The melting points (T_m), melting enthalpy (H_m) and crystallinity (X_c) are listed in Table 1. The melting point of sample 1 (Fig. 1(a)), with inhibitor of the ester-interchange reaction added, was 529 K, which corresponded to folded-chain crystals, the same as the original material. Sample 2 (Fig. 1(b)), pure PET, had two melting points, 529 and 542 K; 529 K was the same as sample 1. The 542 K peak can possibly assigned to the PET extended chain crystal based on

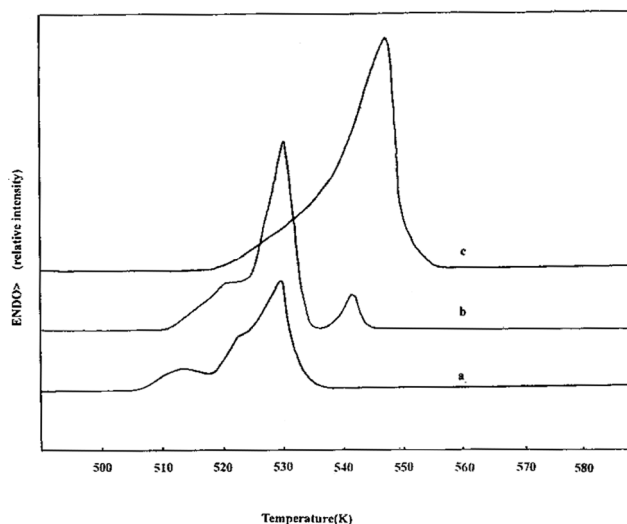


Fig. 1. DSC measurements of the PET samples crystallized at 300 MPa and 573 K for 90 min: (a) sample 1, added inhibitor of transesterification; (b) sample 2, pure PET; and (c) sample 3, added catalyst of transesterification.

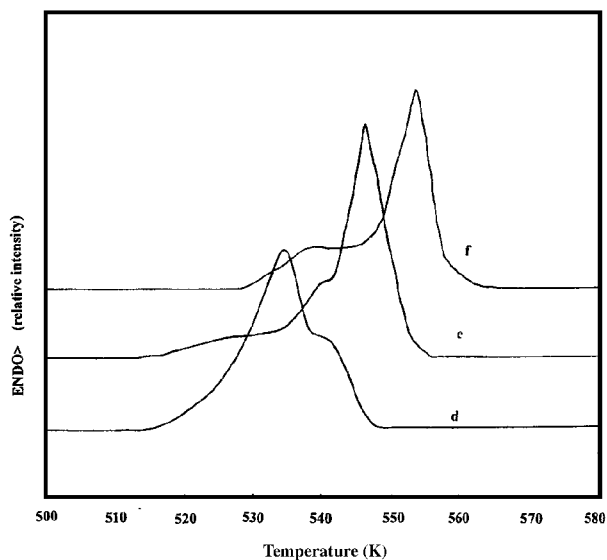


Fig. 2. DSC measurements of the PET samples crystallized at 300 MPa and 603 K for 90 min: (d) sample 4, added inhibitor; (e) sample 5, pure PET; and (f) sample 6, added catalyst.

the results reported by Siegmann [2]. Sample 3 (Fig. 1(c)), with catalyst of transesterification added, demonstrated a high temperature melting point of 544 K, which also possibly corresponded to the PET extended-chain crystals. The peak was wide, especially on the low temperature side. This suggested a wide distribution of thickness of the crystals including some folded-chain crystals. It can be seen that the sample with the added catalyst of transesterification had the highest melting point and enthalpy, while the sample with inhibitor had the lowest; pure PET was in the middle.

According to the simplified Thomson–Gibbs equation [21]

$$T_m = T_m^{\circ} \{1 - [2\gamma / (l\Delta h_f)]\}$$

where T_m° is the melting temperature of the infinitely large crystal, γ the top and bottom specific surface free energy, l

the lamellar thickness, and Δh_f the bulk heat of fusion per cubic centimeter. So a higher melting point (T_m) should correspond to a thicker lamellar crystal. This indicated that the catalyst of ester-interchange reaction can promote PET crystallization by raising the crystallinity and improving the lamellar crystal thickening. On the contrary, the inhibitor of transesterification hindered PET crystallization in these two aspects. This result revealed that the ester-interchange reaction plays an important role in the process of PET crystallization.

Fig. 2 is another illustration of the transesterification effect on PET crystallization. Samples 4–6 were crystallized at 300 MPa and 603 K for 90 min. With catalyst or inhibitor added, sample 4 (Fig. 2(a)) and sample 6 (Fig. 2(c)) showed T_m lower or higher than the pure PET sample 5 (Fig. 2(b)), respectively. This confirmed that the ester-interchange reactions promoted the thickening process of lamellar crystals. Both samples 5 and 6 had a wide shoulder on the low temperature side, while sample 4 had a shoulder on the high temperature side.

Comparing Fig. 1 with Fig. 2, it is obvious that higher crystallization temperature may result in samples with higher atmospheric pressure melting points. This also favored the suggestion that transesterification played an important role in PET crystallization because it was easier for transesterification to occur at higher temperature.

Because PET has a specific band (988 cm^{-1}), which is assigned to folded chains [22], FTIR was also employed to characterize the PET samples. Samples 1–4 had 988 cm^{-1} peaks, although the intensities relative to the 972 cm^{-1} band of samples 3 and 4 were lower. The 988 cm^{-1} band in sample 3 can possibly correspond to the wide low temperature part in the DSC curve; low relative intensity of 988 cm^{-1} in sample 4 possibly indicates that the high temperature shoulder in the DSC curve should be assigned to the extended-chain crystal. Perhaps samples 5 and 6 are also composed of folded chains, but the amount seemed to be too little to be characterized with 988 cm^{-1} band.

Fig. 3 shows two typical TEM photographs of sample 5. We have been unable to obtain electron diffraction data on

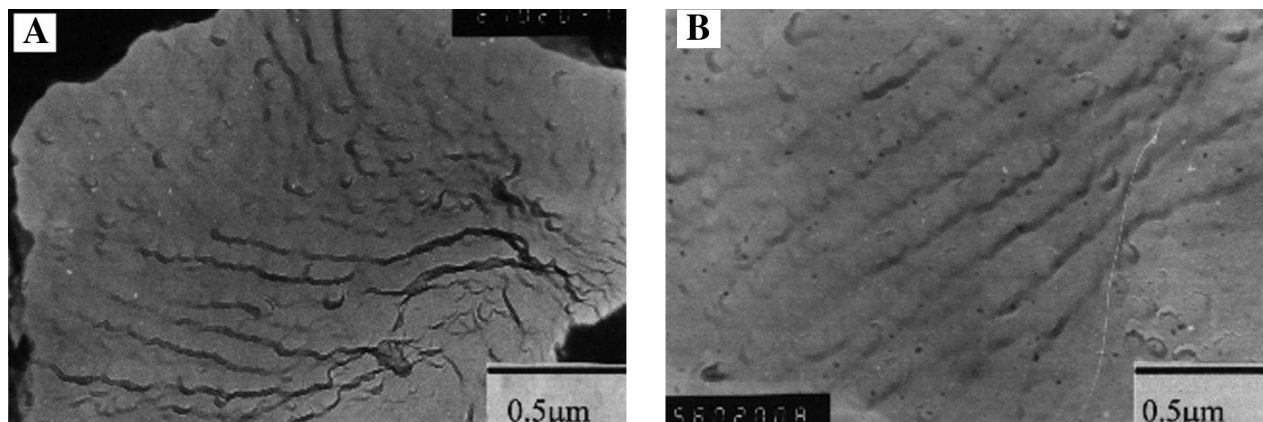


Fig. 3. TEM photographs of sample 5, pure PET crystallized at 300 MPa, 603 K for 90 min.

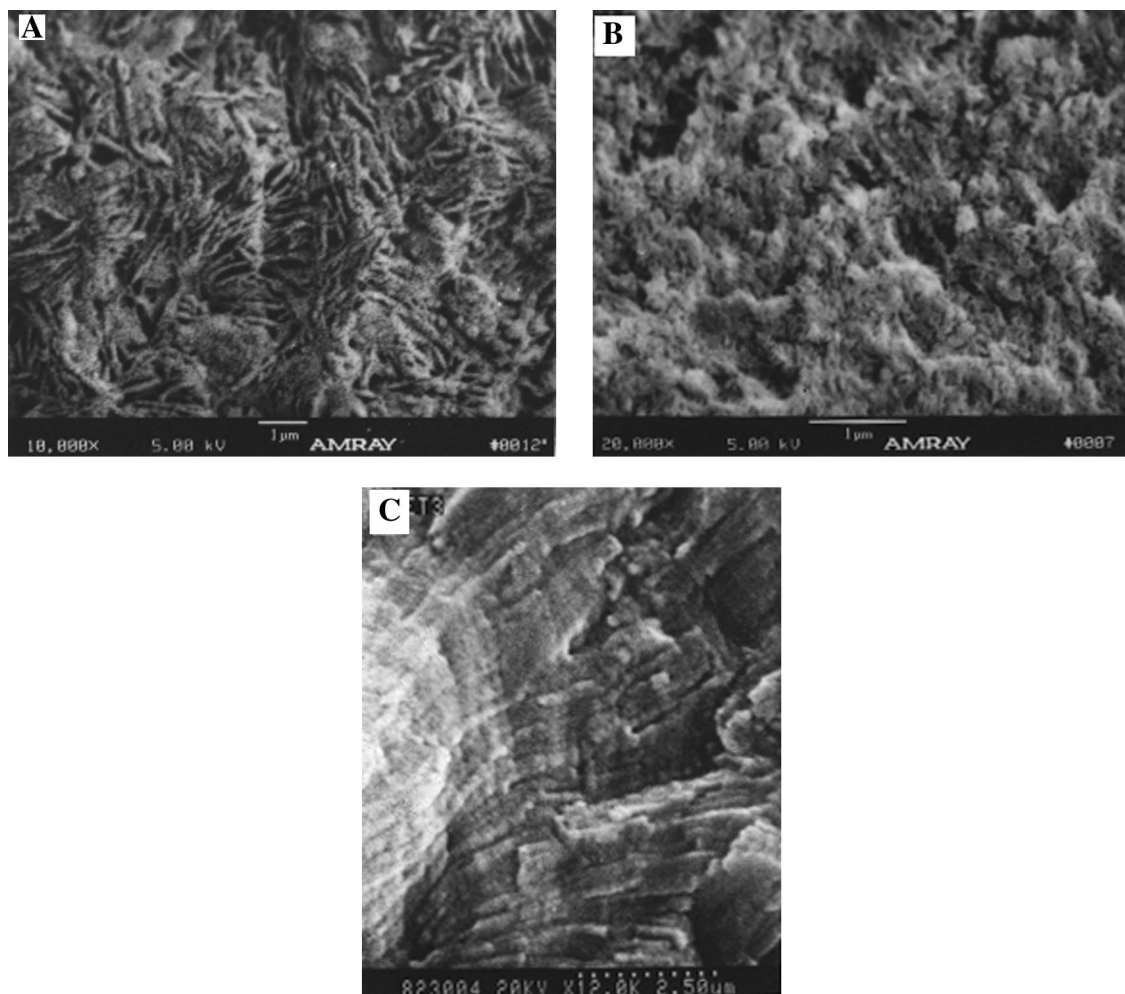


Fig. 4. The SEI of high-pressure crystallized PET samples fracture surface: (A) sample 6, (B) sample 5, (C) pure PET crystallized at 300 MPa and 603 K for 180 min.

any of the samples with Bassett's detachment replica technique [23]. However, based on Anderson's method [24] and Geil's result [25], the striation appearance of the fracture surface of sample 5 in Fig. 3 is the most common feature of the extended-chain crystals. The striations run parallel to the molecular chain direction and the thickness was up to 100 nm, which approximately equaled the average length of the molecular chains. A secondary electron image (SEI) of sample 5 is shown in Fig. 4(A). The striations can also be observed, although it is not very clear. Fig. 4(B) shows a typical SEI of sample 6. It can be seen that the striation appearance is clear. The lamellar thickness was up to 1.5 μm , which is more than 10 times that of the pure PET sample 5 crystallized under the same conditions. Another SEI of a pure PET sample crystallized at 300 MPa and 603 K for 180 min is shown in Fig. 4(C) for comparison. It can be seen that the lamellar thickness of sample 6 with catalyst crystallized for 90 min almost equaled that of the pure PET sample crystallized for 180 min. This is direct evidence for the proposition that transesterification promoted the PET extended-chain crystallization.

Zachmann et al. [15] have suggested that transesterification can promote crystallization through disentanglement. This usually occurs in the molten state or amorphous region as shown in Fig. 5(A). Because the specific folded-chain surface energy is much higher than the specific lateral surface energy, it is easier for strained folds of lamellar crystals to be broken at high temperature, especially with added catalyst. As a result of transesterification, new $-\text{COOC}-$ bonds are formed between the cut chains of the adjacent lamellae that may lead to the chain extension. This model of formation of the extended-chain crystals is shown in Fig. 5(B), which has been also proposed for the polyamides extended-chain crystallization under high pressure [26].

High pressure can ensure the stability of PET at high temperature, which is a necessary condition to offer enough activation energy for transesterification. On the other hand, the distance between lamellar crystals can be reduced drastically during high-pressure crystallization. Stribeck and Zachmann [27] have reported that the distance between lamellar crystals of high-pressure crystallized PET was about 1.3 nm. This is approximately the length of one

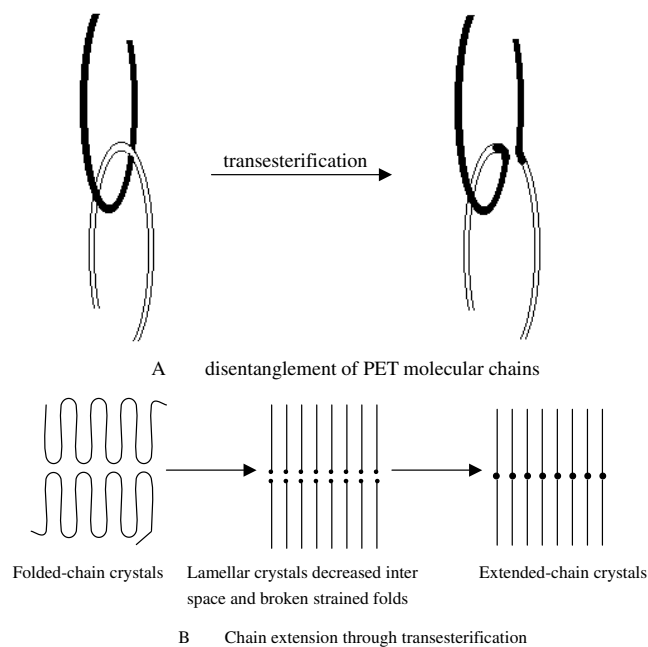


Fig. 5. An illustration of disentanglement and chain extension through transesterification.

chemical repeat unit (1.09 nm). Shorter distance may be expected to increase extensively the incidence of transesterification between adjacent lamella.

Thus we propose that the effect of transesterification on crystallization is different at different crystallization stages. During the primary stage, the effect on disentanglement is more significant and the influence is more apparent in raising crystallinity than in thickening lamella. On increasing the crystallization time, the distance between lamella was reduced to some degree (supposed one or two repeat units), then transesterification becomes primary factor for the thickening process. This suggests that longer crystallization time is a necessary condition for the emergence of high thickening rate.

4. Conclusion

Catalysts and inhibitors of transesterification were added to the PET samples for high-pressure crystallization. The

catalyst promoted the increase of crystallinity and the thickening process of lamellar crystals, while the inhibitor hindered crystallization. This indicates that transesterification can accelerate lamellar thickening and improve the formation of extended-chain crystals.

Acknowledgements

The authors gratefully acknowledge the National Science Foundation Financial support, as well as that of the Ministry of Education foundation. The authors extend their gratitude to Professor Fu Qiang (Department of Polymer Material Science and Engineering) for helpful discussion.

References

- [1] Jog JP. *J Macromol Sci—Rev Macromol Chem Phys C* 1995;35(3):531.
- [2] Siegmund A, Hargett PJ. *J Polym Phys Ed* 1980;18:2181.
- [3] Hiramatsu N, Hirakawa S. *Polym J* 1980;22:105.
- [4] Phillips PJ, Tseng HT. *Macromolecules* 1989;22:1649.
- [5] Konck U, Zachmann G, et al. *Macromolecules* 1996;29:6019.
- [6] Li LB, Li P, Huang R, et al. *J Mater Sci Lett* 1999;18:609.
- [7] Hatakeyama T, Kanetsuna H, Hashimoto T. *J Macromol Sci Phys* 1973;B7:411.
- [8] Hikosaka M. *Polymer* 1987;24:1257.
- [9] Hikosaka M. *Polymer* 1990;31:458.
- [10] Miyagi A, Wunderlich B. *J Polym Sci, Polym Phys Ed* 1972;10:2073.
- [11] Porter RS, Wang LH. *Polymer* 1992;33:2019.
- [12] Fakirov S. *Macromol Chem Phys* 1996;197:2837.
- [13] Fakirov S. *Macromol Chem Phys* 1996;197:2869.
- [14] Fakirov S. *Macromol Chem Phys* 1996;197:2888.
- [15] Kugler J, Gilmer JW, et al. *Macromolecules* 1987;20:1116.
- [16] Mcalea KP, Schultz JM, et al. *Polymer* 1986;27:1581.
- [17] Carduner KR, Carter III, et al. *RO J Appl Polym Sic* 1990;40:973.
- [18] Carduner KR, Carter III RO, et al. *J Appl Polym Sci* 1990;40:976.
- [19] Fu Q, Huang R, et al. *Chin Sci* 1994;A24:1218.
- [20] Starkwhetherer HW, et al. *J Polym Sci, Polym Phys Ed* 1983;21:295.
- [21] Wunderlich B. *Macromolecular Physics*, vol. 3. New York: Academic Press, 1980.
- [22] Hannon MJ, Koenig JL. *J Polym Sci, Polym Phys Ed* 1969;7:1085.
- [23] Bassett DB. *Phil Mag* 1961;6:1053.
- [24] Anderson FR. *J Appl Phys* 1964;35:64.
- [25] Geil P, Anderson FR, Wunderlich B. *J Polym Sci Part A* 1964;2:3707.
- [26] Gogolewski S. *Polymer* 1977;18:63.
- [27] Stribeck N, Zachmann HG, et al. *J Mater Sci* 1997;32:1639.